JOURNAL OF GEOPHYSICAL RESEARCH, VOL. 102, NO. A11, PAGES 24,265–24,281, NOVEMBER 1, 1997

Generation of anomalous flows near the bow shock by its interaction with interplanetary discontinuities

Y. Lin

Physics Department, Auburn University, Auburn, Alabama

Abstract. Two-dimensional hybrid simulations using a curvilinear coordinate system are carried out to study the interaction of the Earth's bow shock (BS) with an interplanetary directional discontinuity. In particular, plasma flow patterns are examined. In the interaction of the bow shock with an interplanetary tangential discontinuity (TD), a bulge of magnetic field and plasma may be present near the intersection between the fronts of the BS and the TD. The bulge expands to the upstream and is embedded in the solar wind. High magnetic field and ion density are present in the boundary regions of the bulge, and the temperature in the bulge is significantly higher than that in the ambient solar wind. A core of low density and sometimes low field is present inside the bulge. The flow speed changes from supersonic in the solar wind to subsonic throughout the bulge. A strong sunward deflection in flow velocity is present both in the bulge and in the magnetosheath behind the bulge. The presence of such hot anomalous flows depends on the direction and symmetry condition of the upstream motional electric field. The formation of the bulge and the associated anomalous flows is found to be mainly due to (1) the reflected ions which are focused to TD under the proper electric field conditions, (2) the unbalanced pressure associated with the geometry change and reformation of the BS which causes the expansion of downstream and the sunward motion of ions, or (3) the occurrence of magnetic reconnection in the current sheet. In the interaction of the BS with an interplanetary rotational discontinuity (RD), the flow may be deflected sunward by the magnetic tension force associated with the resulting rotational discontinuities and slow shocks in the magnetosheath. It is suggested that the observed anomalous flow events upstream of the bow shock may be due to the BS/TD interaction, and both BS/RD and BS/TD interactions may generate strong sunward flow deflections in the magnetosheath.

1. Introduction

Magnetohydrodynamic (MHD) discontinuities and shock waves are often observed in the solar wind [e.g., *Chao and Olbert*, 1970; *Burlaga*, 1971; *Burlaga and Ness*, 1969; *Chao and Lepping*, 1974; *Neugebauer et al.*, 1984; *Richter et al.*, 1985; *Gosling et al.*, 1994; *Whang et al.*, 1996]. Among them, tangential discontinuities (TDs) and rotational discontinuities (RDs) or Alfven waves are most frequently seen [e.g., *Burlaga and Ness*, 1969; *Behannon et al.*, 1981; *Neugebauer et al.*, 1984]. Observations of forward and reverse fast shocks and slow shocks have also been reported [*Chao and Olbert*, 1970; *Russell et al.*, 1983; *Whang et al.*, 1996; *Gosling et al.*, 1994]. At a tangential discontinuity, the normal component of magnetic field is zero, and the normal flow velocity relative to the discontinuity also vanishes. The total pressure is balanced, while the tangential magnetic field and flow may change arbitrarily across the tangential discontinuity. On the other hand, a rotational discontinuity has a finite normal component of magnetic field. In the ideal MHD, the field strength and plasma density are constant across a rotational discontinuity, and the tangential magnetic field may rotate arbitrarily [e.g., *Landau and Lifshitz*, 1960]. The structure of RD and TD in collisionless plasmas has been simulated by many authors [e.g., *Swift and Lee*, 1983; *Lee et al.*, 1989; *Richter and Scholer*, 1989; *Cargill and Eastman*, 1991; *Lin and Lee*, 1993].

The Earth's bow shock (BS) is a fast-mode shock, which is formed by the supersonic solar wind flowing past the Earth's magnetic field [e.g., *Cahill and Patel*, 1967]. Since the bow shock is the first frontier of the plasma environment of the Earth, any interplanetary discontinuities that propagate to the Earth would first encounter the bow shock. The interaction of interplanetary discontinuities with the Earth's bow shock has been one of the very important topics for decades [e.g., *Burlaga and Ogilvie*, 1969; *Brunelli and Grib*, 1973; *Volk and Auer*, 1974; *Neubauer*, 1975; *Burgess and Schwartz*, 1988; *Wu et al.*, 1993; *Yan and Lee*, 1994, 1996; *Lin et al.*, 1996a, b].

Paper number 97JA01989.
0148-0227/97/97JA-01989$09.00

The work presented in this paper is motivated by the companion papers by *Schwartz et al.* [1985, 1988], *Thomsen et al.* [1986, 1988], and *Paschmann et al.* [1988], which report a class of events observed by satellites near the Earth's bow shock. The events are characterized by a large change in plasma flow velocity that for a short period of time has a strong sunward deflection relative to the ambient plasma. The majority of the events are found to be associated with a gross rotation in the interplanetary magnetic field. They have been reported as "plasma structures with anomalous flow directions" [*Paschmann et al.*, 1988, p.11279], "active current sheet in the solar wind" [*Schwartz et al.*, 1985, p.269], and "hot diamagnetic cavities" [*Thomsen et al.*, 1986, p.2961]. Hereafter in this paper, we term the events as "the anomalous flow events." The events have been identified in both upstream near the bow shock and in the magnetosheath [e.g., *Schwartz et al.*, 1988; *Paschmann et al.*, 1988]. The solar wind events usually contain a hot subsonic plasma embedded in the upstream wind, showing a low-density core flanked by narrow regions of high density as well as strong field. The orientations of boundary normals at the leading and trailing edge of the events may be very different.

It has been suggested that the formation of these events is due to the interaction of the bow shock with an interplanetary TD or RD [*Schwartz et al.*, 1988; *Paschmann et al.*, 1988; *Burgess and Schwartz*, 1988; *Burgess*, 1989; *Thomas et al.*, 1991; *Thomsen et al.*, 1988, 1993]. (See also the review paper by *Schwartz* [1995]). The theoretical study by *Neubauer* [1975] has indicated that the discontinuities may "breakup" if the angle between the normal directions of BS and TD is greater than a critical angle. It has been suggested by *Schwartz et al.* [1988] that the breakup of the discontinuities may lead to the formation of a bulge of plasma region on the bow shock and thus a deflection in flow and field. *Paschmann et al.* [1988] have suggested that the interaction of the bow shock with an interplanetary RD may cause an amplification of magnetic stress and thus the generation of bulge structure on the bow shock. They have in addition pointed out that the internal structure of TD may be another candidate to cause the bulge. On the other hand, it has also been proposed that flux transfer events at the magnetopause may also lead to the observed anomalous flow events [*Thomsen et al.*, 1986].

Thomsen et al. [1986, 1988] have shown that many of the events are observed where the geometry of the bow shock is changing and a large fraction of specularly reflected ions are present. The one-dimensional (1-D) hybrid simulation by *Burgess and Schwartz* [1988] have indicated that ion kinetic effects may also be important in the formation of the bulge. Some studies have been conducted for the effects of ion beam instability on a background plasma [*Thomas and Brecht*, 1988; *Onsager et al.*, 1990]. Using a test particle calculation associated with the interaction between the bow shock and a TD, *Burgess* [1989] has shown that the anomalous flows can be formed by specularly reflected ions moving upstream of the bow shock along a certain type of TD, where the motional electric field associated with the upstream bulk flow focuses reflected ions toward the TD from either side of the TD. For other geometries of the electric fields, the ions may interact with the bow shock and cause the modification of the shock. He has also suggested that the TD can deprive a limited spatial region of downstream reflected-gyrating ions and cause the shock to be unstable, which may lead to the injection of a density pulse to the upstream. Further two-dimensional (2-D) hybrid simulations by *Thomas et al.* [1991] indeed show that the structure near the contact locus between the bow shock and a TD may be very different for different types of motional electric fields. A region with high ion temperature, low magnetic field, and low density, can be generated under the "proper" type of the electric field which focuses the reflected ions to the current sheet, whereas no hot flow anomaly is present for motional electric fields directing ions away from the current sheet on both sides of the TD. These simulations and the simulation cases shown by *Thomsen et al.* [1993], however, are carried out for the normal of the bow shock and its upstream flow velocity being parallel to the TD front. Thus there is no relative motion of the TD along the bow shock front, as is quite different from the real situation in which the interaction line moves along the curved bow shock, and the interaction time of the incoming TD with a local bow shock may be short.

The purpose of this paper is to study the generation of anomalous flows by the interaction between the curved BS and an interplanetary TD or RD. According to the general Riemann problem, the interaction between a fast shock and an MHD discontinuity or shock may lead to the generation of up to seven MHD discontinuities and shock waves [e.g., *Gogosov*, 1961; *Jeffrey and Taniuti*, 1964; *Neubauer*, 1976; *Wu et al.*, 1993; *Yan and Lee*, 1994, 1996; *Lin et al.*, 1996a]. The interaction of the bow shock with interplanetary discontinuities has been studied by gasdynamic theory [*Shen and Dryer*, 1972; *Dryer*, 1973], MHD theories for perpendicular shocks [e.g., *Volk and Auer*, 1974], and MHD simulations [*Yan and Lee*, 1996]. One-dimensional MHD [*Wu et al.*, 1993] simulations have been carried out to study the interaction of an interplanetary TD with a perpendicular BS. An additional fast shock or fast expansion wave and a transmitted tangential discontinuity are found to be generated in the interaction, and the bow shock is modified. A solar wind dynamic pressure pulse may be carried by the newly generated fast wave and tangential discontinuity to the Earth's magnetopause. By performing a 1-D hybrid simulation, *Mandt and Lee* [1991] studied the interaction of an impinging fast wave with the magnetopause, which is considered to be a tangential discontinuity to separate the geomagnetic and magnetosheath magnetic fields. Nevertheless, in general, the normal of the local BS may not be in the same direction as the normal of the interplanetary TD. In the framework of MHD theory, the oblique interaction of BS with TD has been investigated by *Neubauer* [1975].

The transmission of Alfven waves through the bow

shock has been studied by an ideal MHD analysis [*Hassam*, 1978]. One-dimensional [*Yan and Lee*, 1996] and two-dimensional [*Yan and Lee*, 1994] simulations have also been carried out to study the interaction of an interplanetary RD or Alfven waves with the bow shock. The simulation shows that as a result of the interaction, a slow-mode-like structure [e.g., *Song et al.*, 1992] with an increase in plasma density and a decrease in magnetic field is present in the magnetosheath near the magnetopause. In addition, *Lin et al.* [1996a, b] have carried out 1-D and 2-D hybrid simulations to investigate the pressure pulses generated in the bow shock and the magnetosheath by the interaction between an interplanetary RD and the bow shock. Two rotational discontinuities, two slow shocks, and a weak fast expansion wave may be generated by the BS/RD interaction. In the 2-D simulation, it is seen that not only a dynamic pressure pulse can be carried into the magnetosheath by the transmitted rotational discontinuities and slow waves, but reflected or backstreaming ions at local bow shock [e.g., *Leroy and Winske*, 1983; *Scholer and Terasawa*, 1990] can also contribute to the generation of pressure pulses both upstream and downstream of the bow shock when a local quasi-parallel shock becomes a quasi-perpendicular shock.

In this paper, we carry out 2-D hybrid simulations using a curvilinear coordinate system similar to that of *Lin et al.* [1996b] to study the interaction of the BS with a directional interplanetary discontinuity. The directional discontinuity may be an RD or a TD across which the magnetic field changes direction but plasma density, flow, and field strength are almost constant. The simulation model is described in section 2. In section 3, we present the simulation results for BS/TD interaction. The results of BS/RD interaction are presented in section 4. A summary is given in section 5.

2. Simulation Model

In the hybrid simulation, the ions are treated as discrete particles, and the electrons are treated as a massless fluid. The 2-D hybrid code used in this study is developed by *Swift* [1995, 1996] and has been used by *Lin et al.* [1996b] to simulate the generation of pressure pulses in the magnetosheath by the interaction of the bow shock with an interplanetary RD.

The 2-D simulation is carried out in the equatorial plane, in which the x axis is assumed to be along the Sun-Earth line and pointing to the Sun, and the y axis is pointing from dusk to dawn. A polar coordinate system is used in the simulation, which consists of the radial distance r in the xy plane, the z axis pointing from north to south, and the polar angle $\theta \equiv \tan^{-1}(x/y)$. The Earth is located at the origin. The simulation domain is within the region with $10\ R_E < r < 35\ R_E$ and $0^o \le \theta \le 180^o$. The inner boundary at $r = 10\ R_E$ corresponds to the magnetopause. The grids are uniformly distributed in the r and θ directions, with a total of 151×122 grids. In the 2-D simulation, the physical quantities are assumed to be uniform in the z direction.

The ion gyrofrequency Ω_0 in the solar wind is chosen to be 0.5 s^{-1}, where $\Omega_0 = eB_0/mc$, B_0 is the magnitude of the unperturbed interplanetary magnetic field (IMF), e is the electron charge, m is the ion mass, and c is the speed of light. This value of Ω_0 corresponds to an IMF $B_0 \sim 5$ nT. The simulation results shown in this paper are for an electron temperature $T_e = 0$. The effects of electron temperature will be discussed elsewhere. In the solar wind, the ion inertial length $\lambda_0 = c/\omega_{pi0}$, where ω_{pi0} is the ion plasma frequency, is chosen to be 0.17 R_E. The grid size along the r direction is $\Delta r = 0.17\ R_E$. The simulations have also been run for a higher spatial resolution with $\Delta r = 0.25\lambda_0$ and $r\Delta\theta \le 0.8\lambda_0$, and the results are similar to those shown in this paper. The Alfven speed in the solar wind is chosen to be $V_{A0} = 0.084\ R_E$/s. The ion plasma beta β_0 in the solar wind is assumed to be 0.5, and the ion gyroradius is about 0.12 R_E in the solar wind. The above value of the ion inertial length is about 10 times of the real value in the solar wind, and the Alfven speed is about 7 times. The relatively large cell size and wind speed in the simulation will allow the calculation to be cost-effective. In our simulation, the number of particles per grid is nearly 40-200. We have also run simulations for different choices of λ_0 and found that the shape and strength of the bow shock are nearly unchanged.

The simulation is performed such that first the bow shock BS is formed by the convection of high-speed solar wind along the $-x$ direction to the Earth. Second, an interplanetary TD or RD is allowed to propagate into the domain toward BS at a certain time after the bow shock is formed. Initially, the solar wind is assumed to be uniform, and the IMF is constant in the simulation domain. The ion temperature is assumed to be isotropic. At $t = 0$, the solar wind starts to pass the obstacle, that is, the semicircular magnetopause. Across the frontside boundary at $r = 35\ R_E$, the solar wind flows and convects the IMF $\mathbf{B_0}$ into the simulation domain. The straight line boundary segments at $\theta = 0^o$ and $\theta = 180^o$ represent two outflow boundaries, respectively. A reflecting wall boundary condition is applied at the inner boundary with $r = 10\ R_E$.

The initial TD and RD are assumed to be a planar 1-D structure that is perpendicular to the xy plane, across which the physical quantities experience a jump only along the discontinuity normal $\mathbf{n}$, which is the propagation direction $\mathbf{k}$ of the discontinuity. The initial discontinuity is allowed to propagate along an arbitrary direction to the bow shock. The TD is an entropy mode discontinuity convecting with plasma, relative to which the plasma flow velocity

$$v_n = 0 \tag{1}$$

where the subscript n indicates the normal component. The normal magnetic field component

$$B_n = 0 \tag{2}$$

The total pressure is balanced across the TD, with

$$P + B^2/2\mu_0 = \text{const} \tag{3}$$

in a plasma with an isotropic temperature, where P is the thermal pressure. In this study, we only consider the interaction of directional discontinuities with BS; that is, we assume that the tangential magnetic field can change direction arbitrarily across the initial TD, but plasma density, pressure, and field strength do not have a significant change. In addition, the flow velocity is assumed to be unchanged across this interplanetary current sheet.

In a plasma with an isotropic temperature, the direction of the tangential magnetic field can change arbitrarily across the rotational discontinuity, while the magnetic field strength and plasma density and pressure remain unchanged. The normal component of inflow velocity at the rotational discontinuity satisfies

$$v_n = \pm B_n/\sqrt{\mu_0 m_i N} \tag{4}$$

where N is the ion number density, m_i is the ion mass, and the positive (negative) sign is applied if the normal incident velocity is parallel (antiparallel) to the normal component of magnetic field B_n. The change of the tangential velocity across the rotational discontinuity should obey the Walen relation

$$\Delta \mathbf{V}_t = \pm \Delta \mathbf{B}_t/\sqrt{\mu_0 m_i N} \tag{5}$$

where $\Delta \mathbf{V}_t$ is the variation of tangential flow velocity across RD, and $\Delta \mathbf{B}_t$ is the change of tangential magnetic field. The normal component of magnetic field

$$B_n = \text{const} \tag{6}$$

at the rotational discontinuity. When RD or TD propagates to various positions, the magnetic field and plasma quantities at the corresponding positions in the frontside semi-circular boundary changes direction. The half width of the initial RD or TD is assumed to be about $2\lambda_0$.

In the calculation, the ions are accelerated by electromagnetic forces. The electric field is determined from the electron momentum equation, and it is then used in the Faraday's law to advance the magnetic field. Quasi-charge neutrality is assumed in the hybrid code. The code utilizes the subcycling of the advance of the magnetic field to the advance of the particle. In our simulation, the time step for the advance of particles is $\Delta t = 0.1\ \Omega_0^{-1}$, and the magnetic field is advanced 10 time steps for every time step the particles are advanced. The magnetic field B is normalized to the unperturbed IMF B_0, ion number density N to N_0, flow velocity V to V_{A0}, and time t to Ω_0^{-1}. The thermal and magnetic pressures are expressed in units of $P_0 \equiv B_0^2/\mu_0$, which is equal to $N_0 V_{A0}^2$.

3. Interaction of an Interplanetary TD With BS

In this section, we present six cases for BS/TD interaction, as indicated in Table 1. In cases 1 and 2, the normal component of the motional electric field relative to the initial TD as inferred from the upstream magnetic field and bulk flow velocity of the bow shock is symmetric on both sides of the TD, either toward or away from the TD. In cases 3 to 6, the magnetic field geometry and the motional electric field are asymmetric on the two sides of TD, and a relatively large modification of the bow shock due to the BS/TD interaction is anticipated [e.g., *Neubauer*, 1975].

3.1. Symmetric Electric Field

In case 1, the initial IMF has an angle of 60° relative to the xy plane, and the field component in the xy plane makes an angle of 45° with the $-x$ and $-y$ direction, with $B_{x0} = B_{y0} = -0.354B_0$ and $B_{z0} = 0.866B_0$. The solar wind is assumed to have a speed of $V_0 = 5V_{A0}$ along the $-x$ direction, which corresponds to an Alfven Mach number $M_A = V_0/V_{A0} = 5$. An interplanetary tangential discontinuity convects into the simulation domain from the front side boundary at $t = 20\ \Omega_0^{-1}$, across which the magnetic field changes direction by $\Delta\Phi_B = 120°$. Behind the initial TD, the magnetic field components are $B_{x1} = B_{y1} = -0.354B_0$ and $B_{z1} = -0.866B_0$, where the subscript "1" indicates quantities behind the TD. Note that the TD propagates with a 45° angle relative to the $-x$ and $+y$ direction. In this case, the x and y components of the magnetic field do not change across the TD but B_z reverses sign. The motional electric field projected to the normal $\mathbf{n}$ of the TD, $E_n \equiv \mathbf{E}_0 \cdot \mathbf{n} = -(\mathbf{V}_0 \times \mathbf{B}_{z0}) \cdot \mathbf{n}$, points toward the TD on both the leading and the trailing side of the TD.

The left, middle, and right columns in Figure 1 show the simulation results at $t = 40$, 60, and 75 Ω_0^{-1}, respectively. Shown in Figure 1 are, from the top, magnetic field vectors in the xy plane, the contours of magnetic field B (in logarithm scales), z component magnetic field B_z, ion number density N, ion flow speed V and thermal pressure P, and streamlines in the xy plane. At $t = 40\ \Omega_0^{-1}$, a bow shock has formed in front of the magnetopause, as indicated in Figure 1. Across the BS the magnetic field, ion number density, and pressure increase, while the flow speed decreases. The flow diverges to the dawn (right) and dusk (left) flank sides. The initial interplanetary TD has propagated near the dusk side BS, as indicated in Figure 1. Note that across the TD the magnetic field lines are aligned with the discontinuity front.

At $t = 60\ \Omega_0^{-1}$, the TD has already interacted with part of the BS on the dusk side and has reached the subsolar region on the shock front of the BS. It appears that similar to the results obtained by *Neubauer* [1975], *Burgess and Schwartz* [1988], and *Wu et al.* [1993], a modified bow shock (BS′) and a transmitted tangential discontinuity (TD′), which appears in the magne-

Table 1. Cases for BS/TD Interaction

	Symmetric **E**	Asymmetric **E**
E toward TD	case 1	case 3
E away from TD	case 2	cases 4, 5, and 6

BS, bow shock; TD, tangential discontinuity.

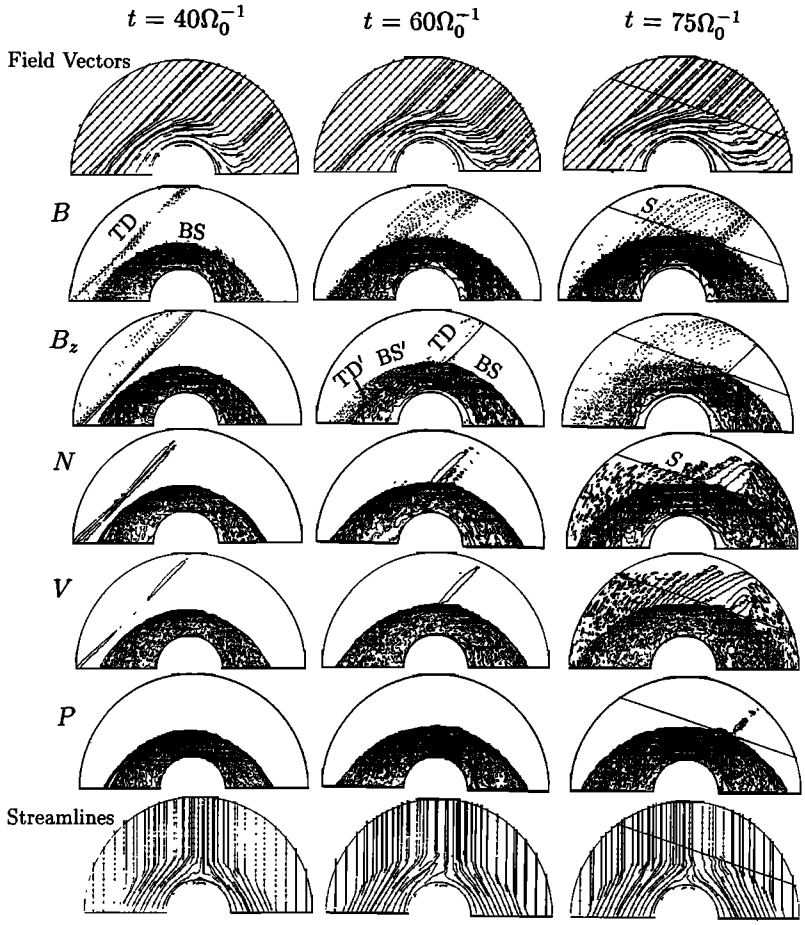

Figure 1. (top to bottom) Magnetic field vectors in the xy plane, contours of magnetic field B, z component magnetic field B_z, ion number density N, ion flow speed V and thermal pressure P, and streamlines in the xy plane at (left) $t = 40\ \Omega_0^{-1}$, (middle) $t = 60\ \Omega_0^{-1}$, and (right) $t = 75\ \Omega_0^{-1}$ obtained in case 1. The straight line S in the right column indicates the path for the profiles in Figure 3.

tosheath as indicated in the middle column of Figure 1, have formed as a result of the interaction between the initial BS and a directional TD. The transmitted fast-mode wave is too weak to be identified. The modified bow shock and the transmitted tangential discontinuity, which propagates to the magnetopause, proceed behind the initial TD as the TD sweeps the BS. The strength of the modified bow shock is nearly the same as that of the original BS. Across the transmitted tangential discontinuity, the field rotates by nearly the same angle as across the initial TD. A detailed analysis for all the wave modes and associated pressure pulses generated through the oblique BS/TD interaction will be given elsewhere.

Note that in our 2-D simulation, the bow shock keeps propagating sunward because of the pileup of magnetic flux at the magnetopause. This systematic motion is slow after the bow shock has formed, with a speed of less than 10% of the upstream flow velocity or the relative speed between the BS and TD. The strength and structure of the BS are nearly not changing with time if without the interaction with the TD. This slightly relative motion between the BS and TD may not have much effect on the simulation, although it results in a slightly higher Mach number of the shock.

At $t = 60\ \Omega_0^{-1}$, a cavity has formed in the contact area between the BS and TD. This cavity appears to be embedded in the downstream plasma of the bow shock, in which the magnetic field and ion number density are below the values of the ambient downstream, similar to the results by *Thomas et al.* [1991]. The temperature increases near the edges of the cavity. Figure 2a shows the ion particle velocities v_{ix}, v_{iy}, and v_{iz} (normalized to V_{A0}) along $\theta = 90^o$, the trailing edge of the cavity, from $r = 17\ R_E$ to $21\ R_E$ at $t = 60\ \Omega_0^{-1}$. Reflected ions are observed at the intersection between the BS and TD near $r = 19R_E$, as shown in the v_{ix} and v_{iy} plots. These ions gain energy from the motional electric field and are accelerated in the $+y$ direction toward the TD. The electric field focuses the hot reflected ions to the current sheet from both the leading and trailing sides. Note that the flow velocity is also deflected from the edges of the cavity toward the current sheet, as shown in the streamline plot in the middle column of Figure 1. The cavity has slightly expanded by this time, and the contact area between the BS and TD is wider than

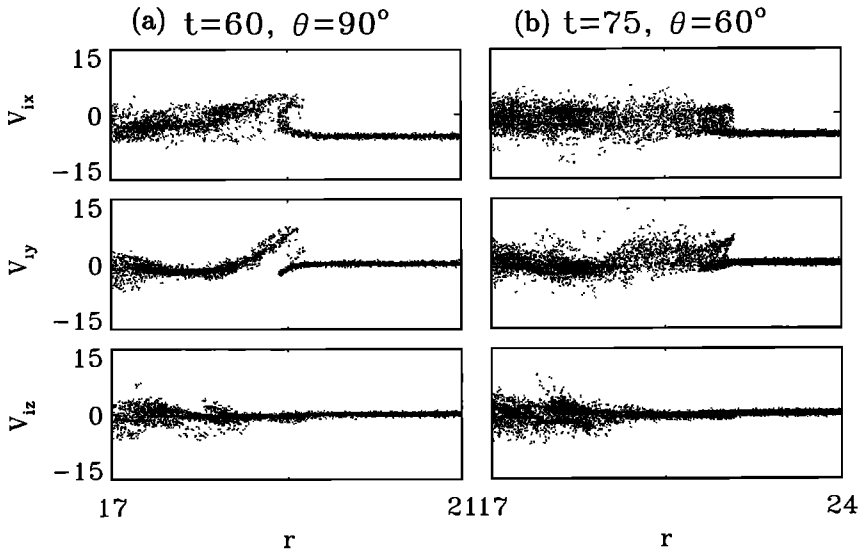

Figure 2. The ion particle velocities v_{ix}, v_{iy}, and v_{iz} (normalized to V_{A0}) as a function of distance r from the center of the Earth (in units of R_E) along (a) $\theta = 90^o$ for $t = 60\ \Omega_0^{-1}$ and (b) $\theta = 60^o$ for $t = 75\ \Omega_0^{-1}$.

the width of the TD. This cavity, however, does not develop as in the cases shown by *Thomas et al.* [1991]. At $t = 60\ \Omega_0^{-1}$, its bottom has reached the resulting TD′ in the downstream region. At the center of the cavity, the temperature is nearly as low as that in the upstream plasma. The flow speed is nearly the same as the upstream inflow speed. This cavity is not in equilibrium.

As the TD further propagates along the surface of BS, hot reflected ions accumulate upstream near the edges of the TD, as predicted by *Burgess* [1989]. Some hot reflected ions are left behind the TD as it propagates, and a bulge of hot ions is formed at the trailing edge of the BS/TD intersection. On the other hand, no bulge appears at the leading side of the TD. The bulge expands to its ambient with time. At $t = 75\ \Omega_0^{-1}$, the TD has propagated to the dawnside ($y > 0$), where the fronts of TD and BS are almost perpendicular to each other and the interaction time between the TD and BS is relatively long. A significant bulge has developed on the BS front at the trailing edge of the TD. The width of the TD becomes quite large near the BS/TD interaction region, spanning the bulge. The bulge stands into the upstream of the BS by about 2 R_E relative to the average front of the bow shock. The bulge structure is found to be localized and moving with the initial TD on the surface of the BS.

Associated with the sunward expansion of the bulge front and the motion of reflected ions is an outward motion of the ion flow. A strong sunward deflection of the flow is seen in the streamline plot in the right column of Figure 1. Figure 2b shows the ion velocities at $t = 75\ \Omega_0^{-1}$ at various locations from $r = 17\ R_E$ to 24 R_E along $\theta = 60^o$ which passes through the bulge region. The bulge region ranges from $r \simeq 20\ R_E$ to 22 R_E along this radial line. The thermal velocities of ions appear more scattered in the bulge region, as seen in Figure 2b. Nevertheless, no strong thermalization appears in the z direction. The perpendicular temperature is much higher than the parallel temperature in the bulge region, as is quite different from the satellite observations which show that the ions are nearly isotropic in the hot anomalous flow events [e.g., *Thomsen et al.*, 1986]. The lack of the isotropic thermalization may be due to the fact that the spatial resolution in the simulation is not high enough for wave instabilities associated with the large temperature anisotropy to develop within the bulge. It may also be due to the 2-D nature of the simulation. The bulge uniformly extends to infinity in the z direction, and there are no wave vectors associated with any instabilities in the z direction. A further study using three-dimensional particle models with more realistic time and spatial scales is necessary.

In order to see the properties of field and plasma quantities in the bulge, here we plot the profiles of the physical quantities at $t = 75\ \Omega_0^{-1}$ as a function of the spatial coordinate θ along part of the path S as indicated in the right column of Figure 1, which passes through the bulge with an angle of 21° relative to the y direction. The left column of Figure 3 shows, from top to bottom, the spatial profiles of the magnetic field components B_r, B_z, B_θ, field strength B, latitudinal angle α_B (dashed line) and azimuthal angle γ_B (solid line) of the magnetic field, flow speed V, latitudinal angle α_v (dashed line) and azimuthal angle γ_v (solid line) of the ion flow, ion number density N, and temperature T. Here α_B (α_v) is the angle between the magnetic field (flow velocity) and the z axis, and γ_B (γ_v) is the angle between the field (flow velocity) projection in the xy plane and the x axis. Note that $\alpha_v = 0^o$ and $\gamma_v = 90^o$ indicates a sunward flow along the $+x$ direction. A close look of the contours of magnetic field, ion number den-

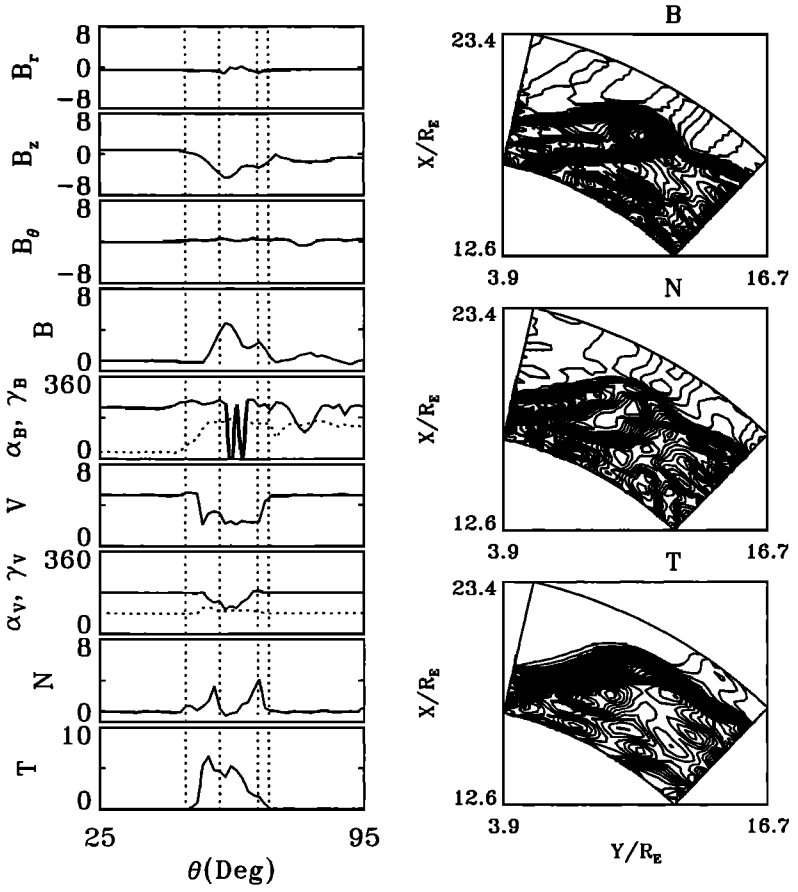

Figure 3. (left) Profiles of the normalized quantities along the path S in Figure 1 as a function of the spatial coordinate θ. (top to bottom) Spatial profiles of the magnetic field components B_r, B_z, B_θ, field strength B, latitudinal angle α_B (dashed line) and azimuthal angle γ_B (solid line) of the magnetic field, flow speed V, latitudinal angle α_v (dashed line) and azimuthal angle γ_v (solid line) of the ion flow, ion number density N, and temperature. The angle α_B (α_v) is the angle between the magnetic field (flow velocity) and the z axis, and γ_B (γ_v) is the angle between the field (flow velocity) projection in the xy plane and the x axis. All the angles are in units of degree. The two vertical dotted lines on each side roughly mark the boundary region of the bulge on that side. (right) Contours of (top) magnetic field, (middle) ion number density, and (bottom) temperature around the bulge region at $t = 75\ \Omega_0^{-1}$.

sity, and temperature around the bulge region is also shown in the right column of Figure 3.

A significant increase in magnetic field and ion number density relative to the ambient upstream is found in the boundary regions of bulge, as seen from the spatial profiles in the left column of Figure 3, where the two vertical dotted lines on each side of the plots roughly define the boundary region on the corresponding side of the bulge. This bulge structure is embedded in the solar wind, which has a low magnetic field, ion number density, and temperature. A plasma region with low density is present at the center of the event, as seen in the profiles of N as well as its contour plot. There also exists a core of low field region in later times, but it is in general not as low as the density. The thickness of the boundary region, where the high density flanks the bulge, and the strength of the associated field and density may be different as one passes through a different part of the bulge. The latitudinal angle α_B of magnetic field changes from 0^o to 120^o, and this field change is usually present on the leading side of the bulge. Large fluctuations in the azimuthal angle γ_B are found throughout the event. The azimuthal angle γ_v of the flow velocity is found to change from 180^o before the event to about 80^o in the bulge region. This change indicates that the flow strongly deviates sunward from its upstream earthward direction. Note that $\gamma_v < 90^o$ represents a sunward component with $V_x > 0$. The ion flow speed is reduced from supersonic in the solar wind to subsonic in the bulge. Many of the above results are consistent with the satellite observations of the upstream anomalous flow events near the bow shock [e.g., *Schwartz et al.*, 1988].

The increase in temperature exists in most part of the bulge region, while this increase is relatively slow at the trailing edge where the high density flanks the center part of the bulge. The temperature increase at the leading edge of the bulge tends to be sharp, as shown in Figure 3, different from the trailing edge where the temperature increases slowly in the high density boundary.

The trailing part of the profile is more consistent with the observations [e.g., *Paschmann et al.*, 1988; *Schwartz et al.*, 1988] than the leading part. A close examination of the simulation results shows that the total pressure at the leading edge is much larger than that in the ambient plasmas, indicating a stronger time variation near the leading edge. In some other cases in which the bulge has further developed, the total pressure there is reduced to a moderate level. In the simulation, little effects of reflected ions are found at the leading edge of the bulge. Note that in the simulation the propagation speed of the TD relative to the curvature of the bow shock front is larger than that in the reality.

As the TD continues to move into the flank side of the BS, the outer boundary of the bulge extends toward the dawnside. The sunward deflection in flow becomes weaker. We have also simulated the cases with the same BS and TD as case 1 but different magnitude of B_{z0}. The results are similar to case 1. For example, a significant bulge also forms in the case with a 70° field rotation angle across the TD. Overall, the strength of the bulge and the associated flow sunward deflection is larger for a larger B_{z0}.

In case 2, the initial BS and TD are similar to that of case 1, except that the sign of B_z is different from that in case 1, with $B_{z0} = -0.866B_0$ ahead of the TD and $B_{z1} = +0.866B_0$ behind TD. The motional electric field is pointing away from the TD on both sides of the current sheet. Figure 4 shows the field lines, streamlines, and contours of physical quantities at $t = 75\ \Omega_o^{-1}$. Similar to the results in case 1, a transmitted tangential discontinuity TD′ is present in the downstream region behind the interaction line.

The structure near the interaction region between the TD and BS, however, is quite different from that in case 1. Instead of the formation of a bulge which stands out of the average bow shock front, at some distance from the interaction region the front of BS′ appears to locate inward toward the downstream, as shown in Figure 4. The bow shock near the interaction region undergoes a reforming and steepening process. This is due to the fact that the motional electric field causes the reflected ions to gyrate away from the TD on both sides of it and thus leads to the lack of downstream gyrating ions. The local bow shock is therefore unstable in a manner similar to that suggested by *Burgess* [1989]. The shock steepens, and more reflected ions are formed near the region. This effect is more evident as the TD is sweeping the bow shock and moving into the dawnside. Behind the interaction line, a bulge-like structure is formed as shown in Figure 4, which contains a hot plasma. A sunward flow deflection is present correspondingly. In later times of the simulation run, this bulge also extends into the upstream. Nevertheless, the overall size of the upstream bulge is not as large as that of case 1.

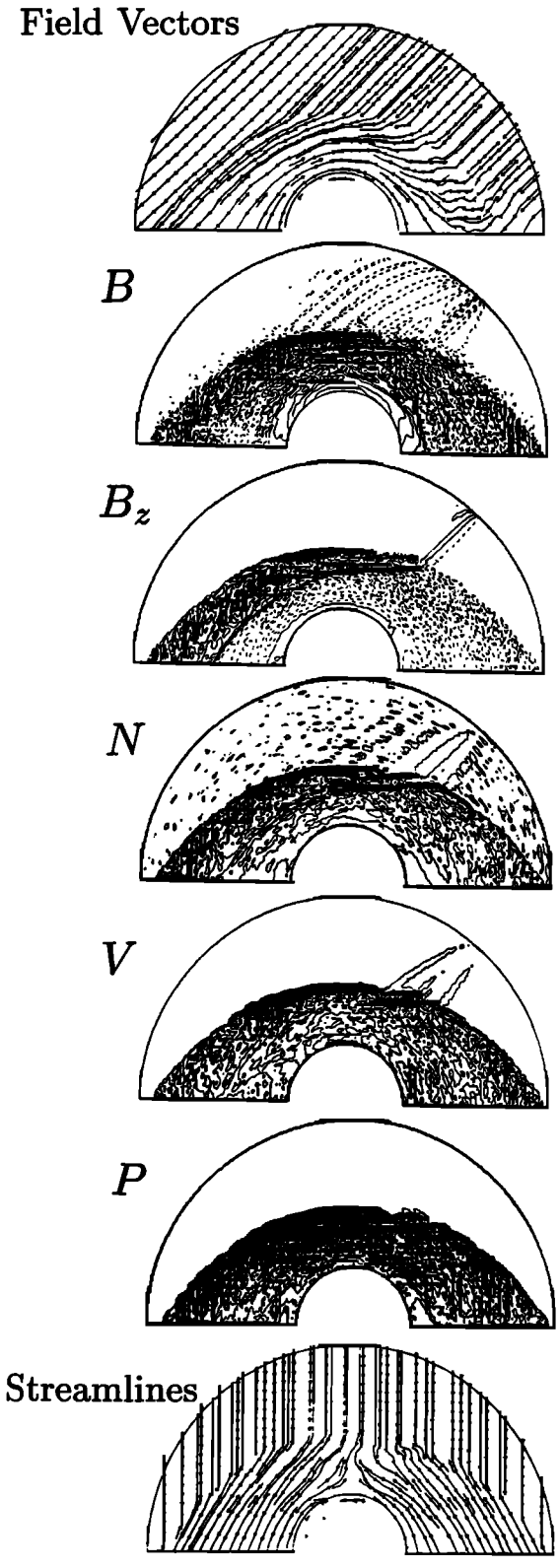

Figure 4. Magnetic field vectors, contours of B, B_z, N, V, and P, and streamlines for case 2 at $t = 75\ \Omega_0^{-1}$.

3.2. Asymmetric Electric Field

In the following cases, the motional electric field on the two sides of the TD is assumed to be asymmetric. In cases 3 to 5, the magnetic field strength, ion number density, pressure, and flow velocity do not change across the initial TD, whereas the magnetic field direction changes. The effects of a small density jump across the TD are shown in case 6.

In case 3, the initial interplanetary magnetic field is in the xy plane with $B_{x0} = B_{y0} = -0.707B_0$, which makes an angle of 45° with the $-x$ and $-y$ directions. The z component magnetic field $B_{z0} = 0$, and the Mach number $M_A = 5$. An interplanetary TD propagates into the domain from the front side at $t = 20\ \Omega_0^{-1}$, across which the magnetic field changes direction by $\Delta\Phi_B = 80°$, and behind the initial TD the magnetic field components are $B_{x1} = -0.12B_0$, $B_{y1} = -0.12B_0$, and $B_{z1} = -0.98B_0$. Behind the TD, the motional electric field has a component pointing toward the current sheet, whereas the electric field is aligned with the surface of the TD front in the region ahead of the TD.

Figure 5 shows the field lines, contours of magnetic field, B_z, N, flow speed V and P, and streamlines at $t = 70\ \Omega_0^{-1}$. The result of this case is very similar to that of case 1. Behind the TD, the reflected ions near the bow shock are focused to the TD by motional electric field. This effect then leads to the formation of the bulge at the intersection between the TD and BS. The bow shock BS in the dawn region is a quasi-parallel shock and appears more turbulent than that in the dusk region.

One of the differences between case 3 and case 1 is that the bow shock BS′ has been strongly modified after the BS/TD interaction. The magnetic field is mainly in the z direction behind the TD, whereas it is in the xy plane ahead of it. The shock normal angle, $\theta_{Bn} \equiv \cos^{-1}(B_n/B)$, at any local bow shock along BS′ front has changed greatly as compared with that at BS before the interaction. The modification of the bow shock is found to also contribute to the formation of the bulge. This effect is discussed in the following for case 4.

In case 4, the initial bow shock BS is the same as that in case 3. The initial TD is also similar to that in case 3, except that the rotation of the tangential magnetic field is in the sense opposite to that in case 1. The magnetic field components behind the TD are $B_{x1} = B_{y1} = 0.12B_0$ and $B_{z1} = 0.98B_0$, corresponding to a field rotation of $\Delta\Phi_B = -80°$. The motional electric field is pointing away from the TD on its trailing side and aligned with the TD front on its leading side.

The left, middle, and right columns in Figure 6 show the simulation results at $t = 40$, 60, and $70\ \Omega_0^{-1}$, respectively. At $t = 40\ \Omega_0^{-1}$, the initial interplanetary TD has propagated near the dusk side BS, as indicated in Figure 6. The B_z component increases across the TD. At $t = 60\ \Omega_0^{-1}$, the TD has reached the subsolar region of the BS. A modified bow shock BS′ and a transmitted tangential discontinuity TD′ have formed behind the interaction line.

As seen in Figure 6, the front of the modified bow shock BS′ shifts sunward relative to the BS, consistent with the calculation by *Neubauer* [1975]. This change in the flaring angle of the shock front is due to the oblique interaction between the BS and TD, while the outward shift of the bow shock front is larger for a larger asymmetry in magnetic field on the two sides of the TD. The bow shock BS′ becomes a nearly perpendicular shock after the interaction. The same case has been run

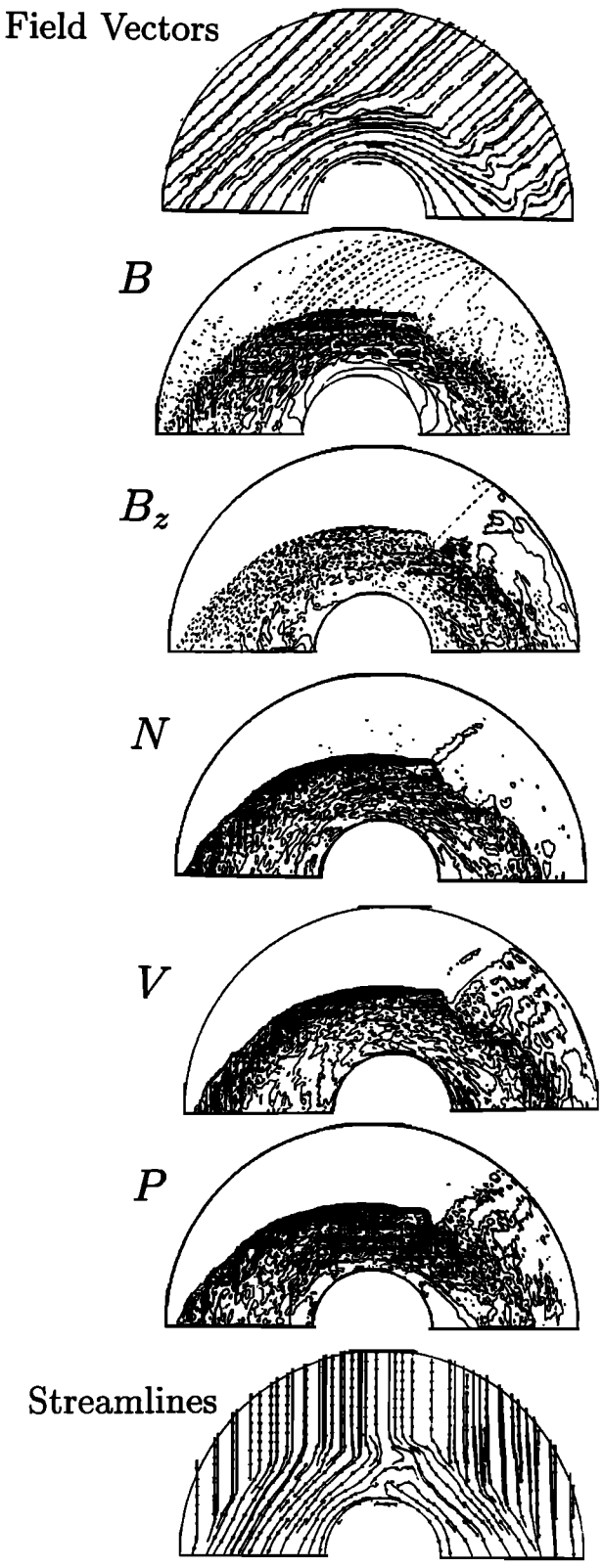

Figure 5. Field lines, contours of magnetic field, B_z, N, flow speed V and P, and streamlines at $t = 70\ \Omega_0^{-1}$ for case 3.

with a higher spatial resolution of $\Delta r = 0.25\lambda_0$, and the results are very similar to those shown in Figure 6.

At $t = 70\ \Omega_0^{-1}$, the interplanetary TD has propagated to a position in the dawnside region of BS, where

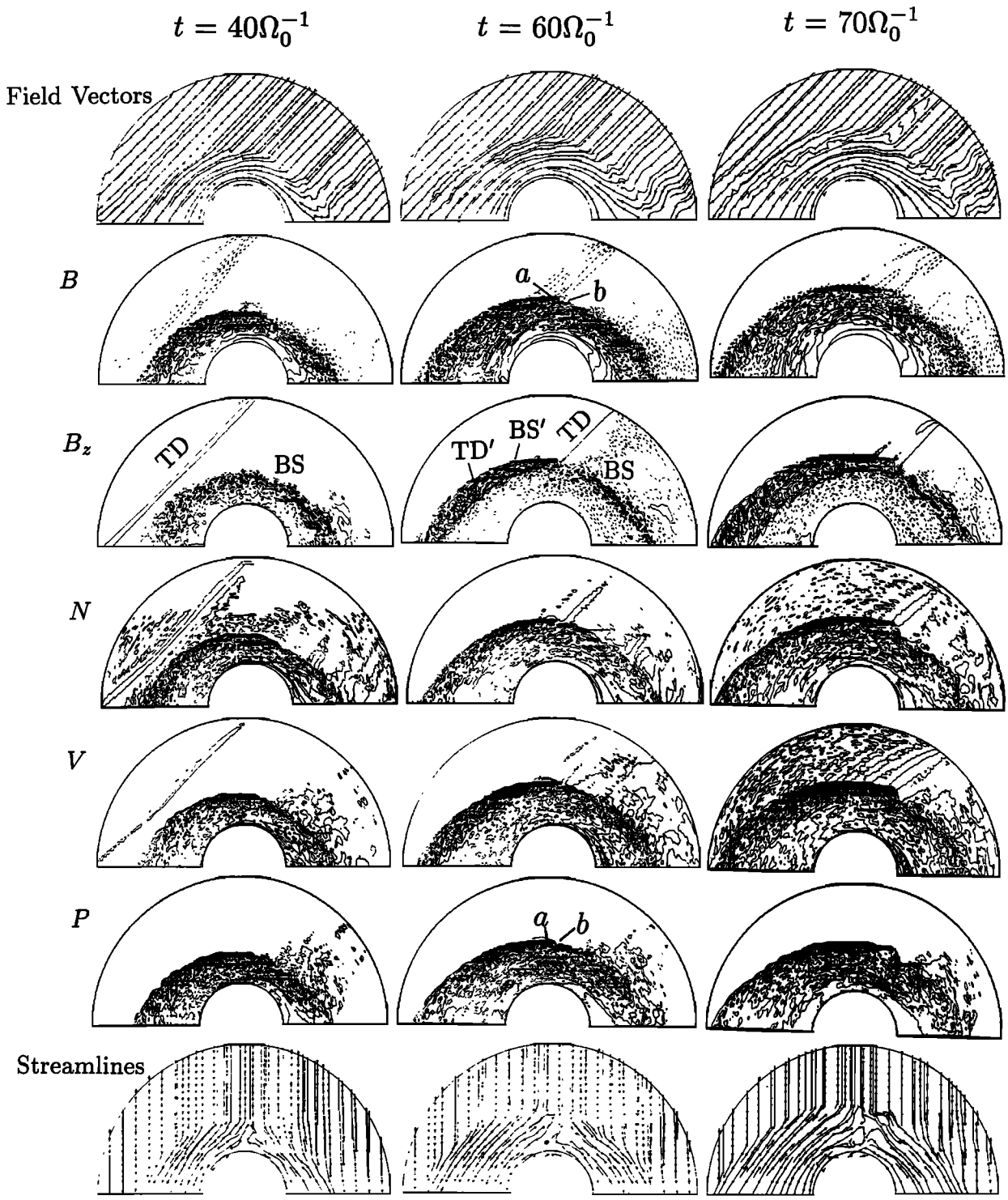

Figure 6. Magnetic field vectors, contours of various quantities, and streamlines at (left) $t = 40\ \Omega_0^{-1}$, (middle) $t = 60\ \Omega_0^{-1}$, and (right) $t = 70\ \Omega_0^{-1}$ obtained from case 4.

the fronts of TD and BS are almost perpendicular to each other. At the intersection between the two fronts, a bulge of magnetic field and plasma has formed, as shown in the right column of Figure 6. The field lines in the bulge is bent toward the upstream. The magnetic field is fairly turbulent in both the interplanetary TD and the TD'. Associated with the sunward expansion of the bulge front is an outward motion of the ion flow. A strong sunward deflection of the flow is seen in the streamline plot. The flow deflection is found both in the bow shock and in the magnetosheath plasma right behind the bulge. Notice that the flow event in the magnetosheath is not in the transmitted tangential discontinuity TD'.

In this case, the formation of the bulge is found to be caused mainly by the modification of the bow shock in

the BS/TD interaction, that is, the difference between the BS ahead of the interplanetary TD and the BS′ behind the TD. Across the contact area of the TD and the BS, the front of the BS′ is at a larger distance from the magnetopause than that of the BS. The magnetic field, ion number density, and pressure at point a immediately downstream of the BS′, as shown in the middle column of Figure 6, are much larger than the field and plasma quantities at point b just upstream of the BS. The plasma and field become discontinuous from a to b. The magnetic field at point a is nearly 3.3 times of that at point b, and the thermal pressure at point a is nearly 51.1 times. The sum of the thermal and magnetic pressures at point a is roughly the same as that in the part of TD′ between a and b, but it is nearly 24 times larger than the total pressure at point b. Since the plasma flow at point b is nearly along the $-x$ direction, there is nearly no normal flow component at the part of discontinuity between a and b and thus no dynamic pressure to balance the difference between the pressures at a and b. The plasma in TD′ thus expands toward point b. At the same time, the motional electric field behind the TD causes reflected ions to move away from the TD. The local bow shock becomes unstable, and the downstream plasma behind the contact area of the BS and TD also expands sunward during the reformation of the bow shock.

Figure 7 shows the contours of magnetic field, ion density, and temperature around the interaction region between the BS and TD at an early time of the bulge formation of case 4. The calculation for this plot is performed for case 4 but with a higher spatial resolution of $\Delta r = 0.25\lambda_0$ and a correspondingly smaller time step. The initial TD is also assumed thinner, with a half width of $1.5\lambda_0$. The presence of the bulge-like structure is clearly seen in Figure 7 between the two different parts of the bow shock front which has different standoff positions. The plasma is found to expand sideways from the center of the bulge. At this moment, the density near the right boundary is much higher than that in the inner area of the bulge. For the initial IMF orientation in case 4, which may represent an IMF in the typical Parker spiral, the unbalanced pressure becomes more significant as the initial TD propagates to the dawn side where the angle between the fronts of BS and TD is large. The sideway expansion is followed by a sunward motion of the downstream ions behind the bulge, leading to the formation of the large bulge in the right column of Figure 6 and the associated sunward flow. Note that as the front of the TD is nearly perpendicular to the front of the BS, the interaction time between the TD and BS is relatively long and the bulge may be more significant.

Another important factor that may contribute to the formation of the bulge is the presence of disturbances in the tangential discontinuity as it collides with the bow shock, as seen in case 4. The disturbances may cause the diffusion of magnetic field and thus a magnetic reconnection. The presence of magnetic reconnection and its effects are discussed below for case 5.

In case 5, the initial BS and the incoming interplanetary TD are the same as those in case 4, except that the field rotates by an angle of 120° across the TD, in the same sense as in case 4. The TD propagates into the simulation domain at $t = 10\ \Omega_0^{-1}$. The left, middle, and right columns of Figure 8 show the field vectors, streamlines, and contours of B, N, and V at $t = 50$, 60, and 70 Ω_0^{-1}. The projection of field lines in the xy plane reverses sign across the TD, as seen in Figure 8. When the incoming TD first collides with the dusk side BS, the current sheet (TD) is compressed, and a local magnetic field line reconnection is found to take place at the interaction site. At $t = 50\ \Omega_0^{-1}$, perturbations and some reconnection in field lines are seen in the transmitted tangential discontinuity TD′, as shown in the field vector plot in the left column of Figure 8.

At $t = 60\ \Omega_0^{-1}$, the interplanetary TD has moved past the subsolar point on the bow shock. A bulge is present at the intersection between the incident TD and the BS. In addition, a clear magnetic reconnection is seen at the intersection. Because of the strong field kink, the ion flow is accelerated by magnetic tension force to the upstream of the bow shock. A flow reversal which is stronger than that in case 4 is found at X line, as shown in the streamline plot in the middle column of Figure 8. The variation of bulk flow velocity due to

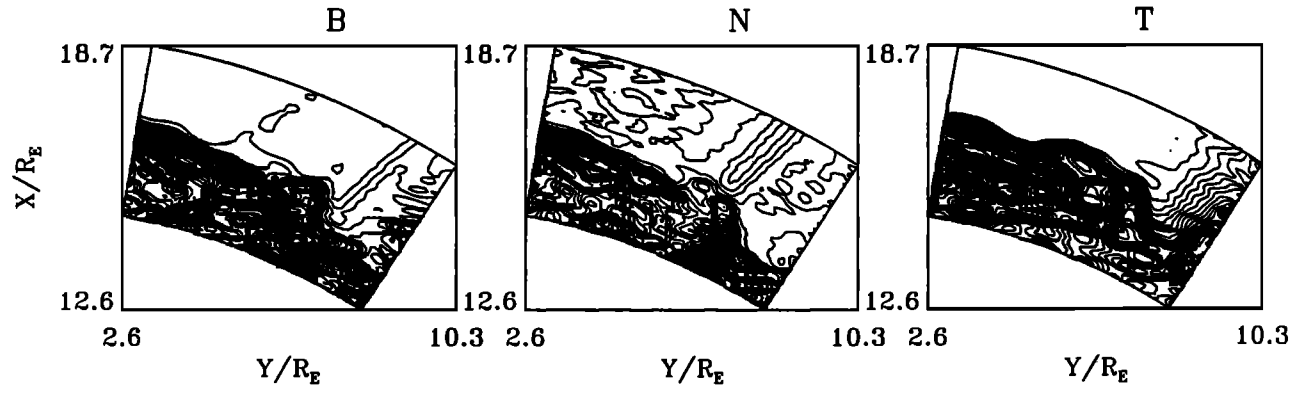

Figure 7. Contours of B, N, and T around the bulge region at an early time while the bulge starts to form. Shown for a run of case 4 with a higher spatial resolution.

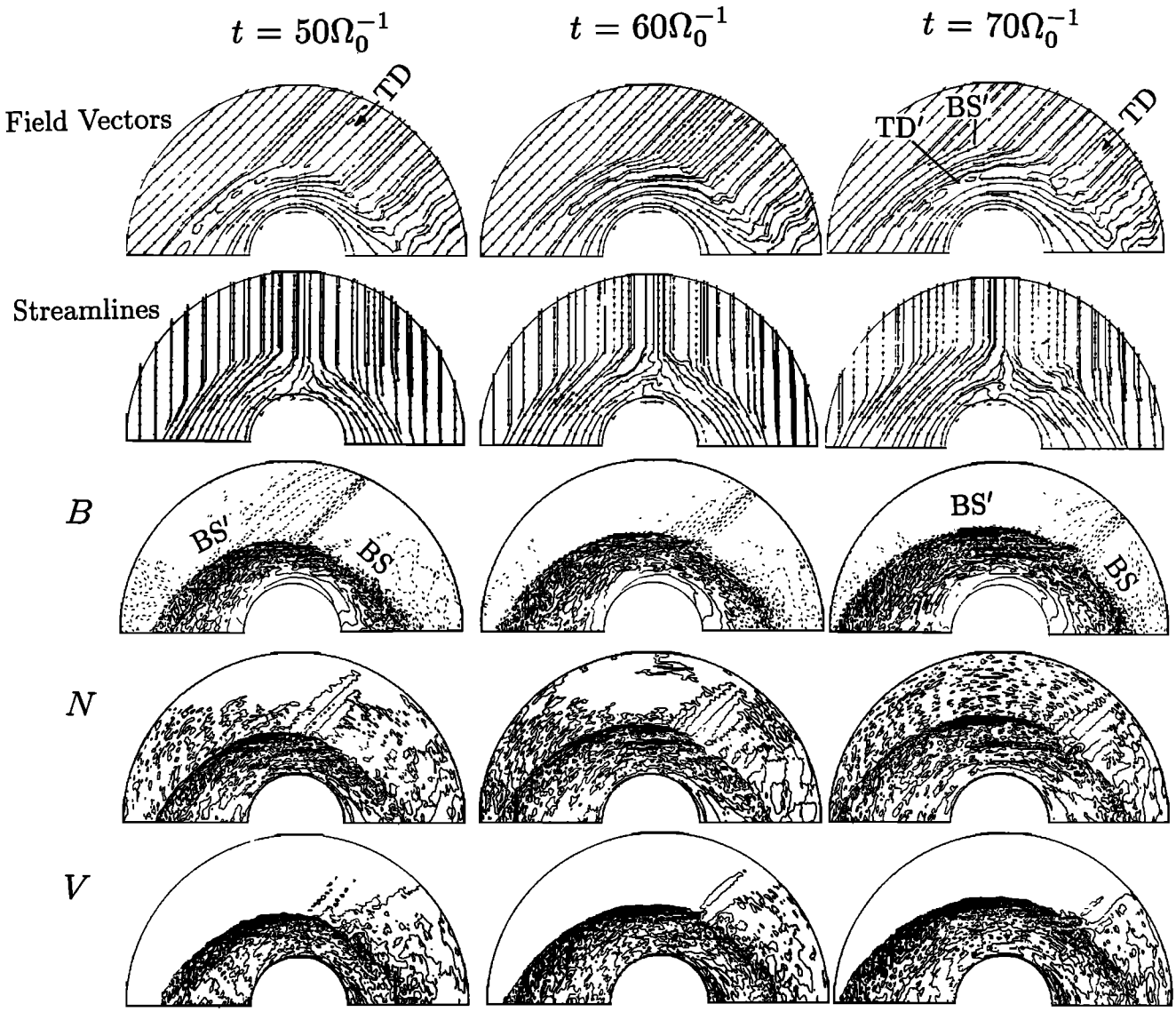

Figure 8. Magnetic field vectors, streamlines, and contours of B, N, and V at $t = 50$, 60, and 70 Ω_0^{-1} for case 5.

reconnection is found to be more apparent when the interplanetary TD has propagated to the dawn side. At $t = 70\ \Omega_0^{-1}$, the incident TD has propagated to the dawn side flank of the BS. Because of the reconnection at the intersection of the initial TD and BS, some of the plasma is ejected from the bow shock to the upstream, as seen from the contour plots of ion number density and flow speed. A filament of high-density ions is found around the reconnection region. Again, a large sunward deflection appears in the flow both at the bow shock and in the magnetosheath, as seen in the streamline plot.

A small background resistivity, which corresponds to a collisional frequency of 0.08 Ω_0, is imposed in case 5. We have also simulated a case with a current-dependent resistivity. The reconnection pattern and the resulting flow pattern are very similar to that shown in Figure 8. The reconnection process is found to be mainly determined by the driving force associated with the compression of the current sheet during the BS/TD interaction.

For cases with the same initial BS (IMF in the xy plane) and the same field rotation sense across TD as in case 4, the simulation of BS/TD interaction has also been carried out for TDs with a field rotation angle $\Delta\Phi_B = -40^o$, -60^o, -90^o, -150^o, -160^o, and -180^o. The bulge and the corresponding flow event are too weak to be identified for the field rotation angle which is less than 40^o. The modification of the bow shock by BS/TD interaction is stronger as $|\Delta\Phi_B|$ increases, and the flow events are also stronger. For the rotation angle which is greater than 80^o, the enhancement of sunward deflection in plasma flow by local magnetic reconnection is clearly seen. Tangential discontinuities with a very large field rotation angle, however, may be rarely seen in the solar wind.

The bulge structure may be enhanced if there exists a density and field jump across the initial TD. Figure 9 shows the simulation results of case 6, in which the initial BS and TD are the same as those in case 4, ex-

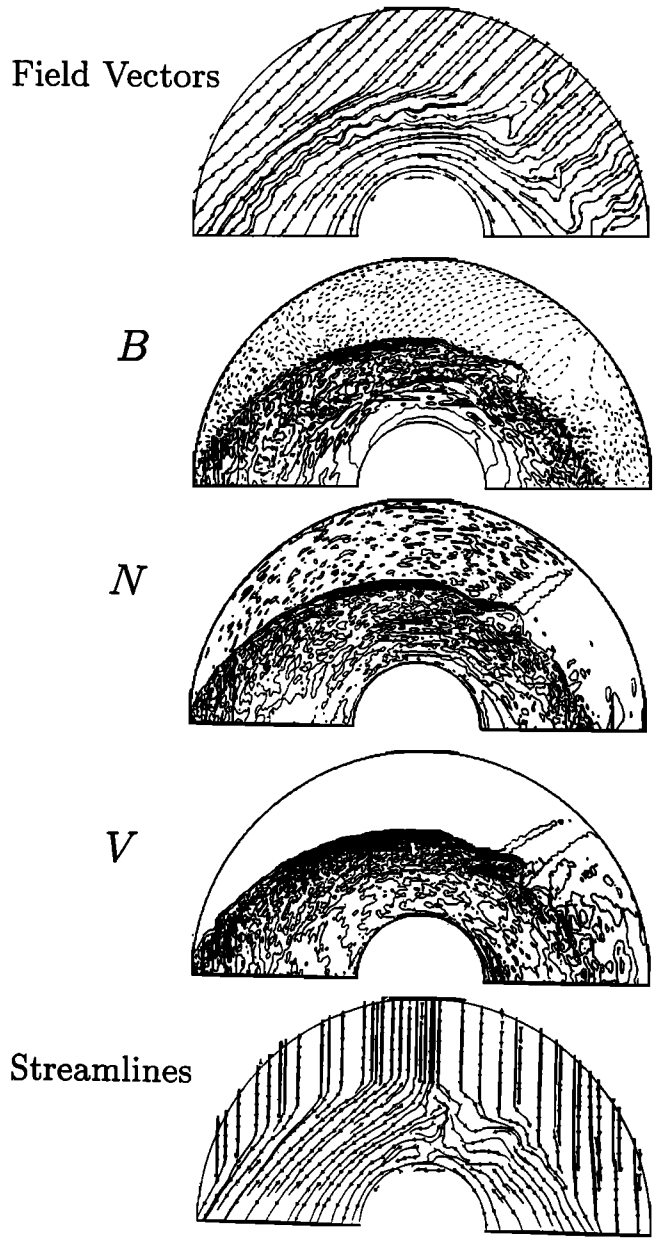

Figure 9. Field vectors, contours of magnetic field, ion number density and flow speed, and streamlines at $t = 70\ \Omega_0^{-1}$ in case 6.

cept there is an ion number density jump $R_N = 0.8$ across the TD. Here $R_N \equiv N_1/N_0$, and N_1 and N_0 are the ion number density behind and ahead of the TD, respectively. Correspondingly, the magnetic field strength is slightly increased across the TD to satisfy the total pressure balance, whereas the temperature is assumed to be constant. The TD is assumed to propagate into the simulation domain at $t = 10\ \Omega_0^{-1}$. Shown in Figure 9 are the field vectors, contours of magnetic field, ion number density and flow speed, and streamlines at $t = 70\ \Omega_0^{-1}$. The bulge at the bow shock is found to be larger than that in case 4. A large sunward deflection in the flow is observed, as shown in Figure 9.

The modification of the bow shock after the BS/TD interaction is stronger than that in case 4. The outward shift of the BS′ front relative to the BS is enhanced by the density ratio $R_N < 1$. In the upstream region of the modified bow shock BS′, the ion number density is smaller than the density upstream of the unperturbed BS, and the the field is slightly larger. The Alfven speed upstream of BS′ is thus increased. Since the flow velocity is unchanged across the initial TD, the Alfven Mach M_A of the bow shock is reduced. A decrease in M_A and dynamic pressure causes the front of the bow shock to move sunward, especially in the flank region. This can also be understood by considering the change in upstream ramp pressure due to the incoming TD. This effect thus strengthens the effects of a net $\Delta\Phi_B$ across the TD as in case 4. As a result, the bulge is larger then that in the $R_N = 1$ case, and so is the flow deflection.

We have also simulated a case which has an $R_N = 1.5$ and otherwise the same as case 6. The bulge is found to be smaller than that in cases 4 and 6. This result may be due to that an $R_N > 1$ leads to an inward shift of the bow shock front, which in this case is against the effects of $\Delta\Phi_B$.

The generation of the bulge structure at the bow shock by BS/TD interaction has been suggested by *Schwartz et al.* [1988]. Apart from the ion kinetic effects, they have also discussed the breakup of the bow shock which is due to an large angle between the fronts of BS and TD. The motion of the interaction line between the BS and TD is slowed down if the angle between their fronts is large. When the angle is greater than a critical angle, the resulting discontinuities in the BS/TD interaction would propagate ahead of the interaction line. This would lead to the breakup of the discontinuities [*Neubauer*, 1975]. Such a breakup, however, has not been identified in our simulation.

It has also been suggested by *Paschmann et al.* [1988] that the internal structure of the TD, such as a filament of low density plasma in the transition of TD, may result in changes in dynamic pressure and Mach number upstream of the bow shock. This modified upstream condition may then cause a deflection of the bow shock. In our simulation, slight variations in density are present inside the TD transition. The upstream condition at local BS is changed by this internal TD structure especially when the fronts of the BS and TD are perpendicular to each other. This change, however, is relatively small and may not be the main reason for the formation of the bulge structure. Some diffusion and expansion are found associated with the incident TD in our simulations as it propagates to the bow shock, but these changes are relatively small, although the width of the TD has effects on the size of the bulge. Nevertheless, we have not simulated the cases with a special internal structure of TD.

It should be noticed that in cases 4 to 6, the electric fields are not toward the TD as in cases 1 to 3. The results in cases 4 and 5 suggest that the bulge may also be present under a largely asymmetric electric field at TD which causes a geometry change of the bow shock even though the electric field is not in the "proper" sense. This result seems to be in contrast to the claim

of *Thomas et al.* [1991], in whose simulation the TD is perpendicular to the straight bow shock front and propagates in the direction of bow shock normal, which is quite different from the realistic situation. While the present simulation has suggested some additional mechanisms for the formation of the bulge, more detailed searches for the structure and size of the bulge under various electric field conditions need to be conducted in future simulations.

4. Interaction of an Interplanetary RD With BS

The simulation has also been carried out for the interaction between the BS and an interplanetary rotational discontinuity. For the cases in which the RD has a small normal component of magnetic field B_n, small bulge-like plasma structure is present at the intersection between the RD and BS in a similar manner as in the TD/BS interaction. The modification of the bow shock position due to the interaction also appears in the BS/RD interaction. Nevertheless, no strong bulge and no apparent flow deflection is found to finally form upstream of the bow shock, which is more evident in the cases with a larger normal component of magnetic field at RD. This result may be due to the fact that a finite normal component of magnetic field at the contact locus between the BS and RD would act to confine the ions to the downstream region. A strong sunward flow deflection, however, can be generated in the magnetosheath by the BS/RD interaction.

We show in case 7 the interaction between the bow shock and an interplanetary rotational discontinuity. A detailed analysis for the BS/RD interaction in the 2-D hybrid model has been given by *Lin et al.* [1996b].

In case 7, the initial IMF is in the $-y$ direction, with $B_{x0} = B_{z0} = 0$ and $B_{y0} = -B_0$. The solar wind flow velocity $V_0 = 5V_{A0}$ along the $-x$ direction. At $t = 30\ \Omega_0^{-1}$, an interplanetary RD propagates to the bow shock from the dawn side front boundary. The propagation direction of the RD is oblique to the x axis, with $\mathbf{k} = (-0.866, -0.5, 0)$, which makes an angle of 30^o with Sun-Earth line. The rotation angle of the tangential magnetic field is $\Delta\Phi_B = -160^o$ across the RD.

The left and right column of Figure 10 shows magnetic field vectors in the xy plane, streamlines in the xy plane, and contours of magnetic field, ion number density, and flow speed at $t = 55\ \Omega_0^{-1}$ and $70\ \Omega_0^{-1}$, respectively. At $t = 55\ \Omega_0^{-1}$, the RD has interacted with the BS in the subsolar region and in most of the dawn side flank region. Kinked field lines are present slightly downstream of the now bow shock BS′. The strength of the BS′ is nearly the same as that of the initial BS. Associated with the field kinks, a strong acceleration or deceleration in ion flow is found. In some regions the streamlines are strongly deflected duskward and sunward, as shown in the left column of Figure 10. The deflection of the flow is also seen at the bow shock front, but it is not as significant as in the cases of BS/TD interaction.

At $t = 70\ \Omega_0^{-1}$, the structure with the field kinks has propagated farther downstream. As obtained by *Lin et al.* [1996a, b], this structure (RD1) is essentially a combination of rotational discontinuities and slow shocks. Inside this structure, the magnetic field decreases, while the ion density and thermal pressure slightly increase. This structure has also been found by *Yan and Lee* [1994, 1996], who have suggested that the propagation of this structure to the magnetopause may lead to the formation of a slow-mode structure [e.g., *Song et al.*, 1992] observed by satellites in the magnetosheath near the magnetopause. The magnetic field rotates by nearly the same angle across RD1 as across the initial RD. A large flow deflection is present in RD1 in the magnetosheath proper, as shown in the right column of Figure 10. A significant dynamic pressure pulse is present in RD1.

The deflection of the magnetosheath flow increases with the field rotation angle $\Delta\Phi_B$ across the initial RD for $|\Delta\Phi_B| \leq 180^o$. We have also simulated cases with various propagation direction $\mathbf{k}$ of the initial RD. The RDs with a propagation direction more oblique to the x axis may result in a larger sunward deflection in flows at the bow shock and in the magnetosheath. This is because that the changes of field direction and velocity at a rotational discontinuity are transverse to the normal direction of the discontinuity. An oblique RD may result in a relatively oblique RD1 front, in which the magnetic tension force may have a relatively large sunward component. Therefore a strong sunward deflection may be generated in the magnetosheath. Note that the generation of anomalous flows in the magnetosheath by BS/RD interaction has also been suggested by *Yan and Lee* [1996].

5. Summary

In summary, 2-D hybrid simulations using a curvilinear coordinate system have been carried out to investigate the generation of anomalous flow events near the bow shock and in the magnetosheath. The interaction between the bow shock and a interplanetary tangential discontinuity or rotational discontinuity is examined. The main results are given below.

In the interaction of the BS with a directional TD, a modified bow shock BS′, a transmitted tangential discontinuity TD′, and some other waves modes may be generated behind the interaction line. The TD′ propagates in the magnetosheath toward the magnetopause. A weak-fast mode wave may also be formed and propagate ahead of the TD′, but it is too weak to be identified. Across the TD′, the rotation angle of magnetic field is almost the same as that across the incident TD. As the interplanetary TD moves to a position where the fronts of BS and TD are nearly perpendicular to each other, a bulge structure of magnetic field and plasma may be formed at the intersection of the BS and TD, in which a hot plasma is present. This bulge expands to the upstream, and the width of the TD near the bulge becomes thick. The size of the bulge, which can be of the order of a few Earth radii, is also related to the thickness of

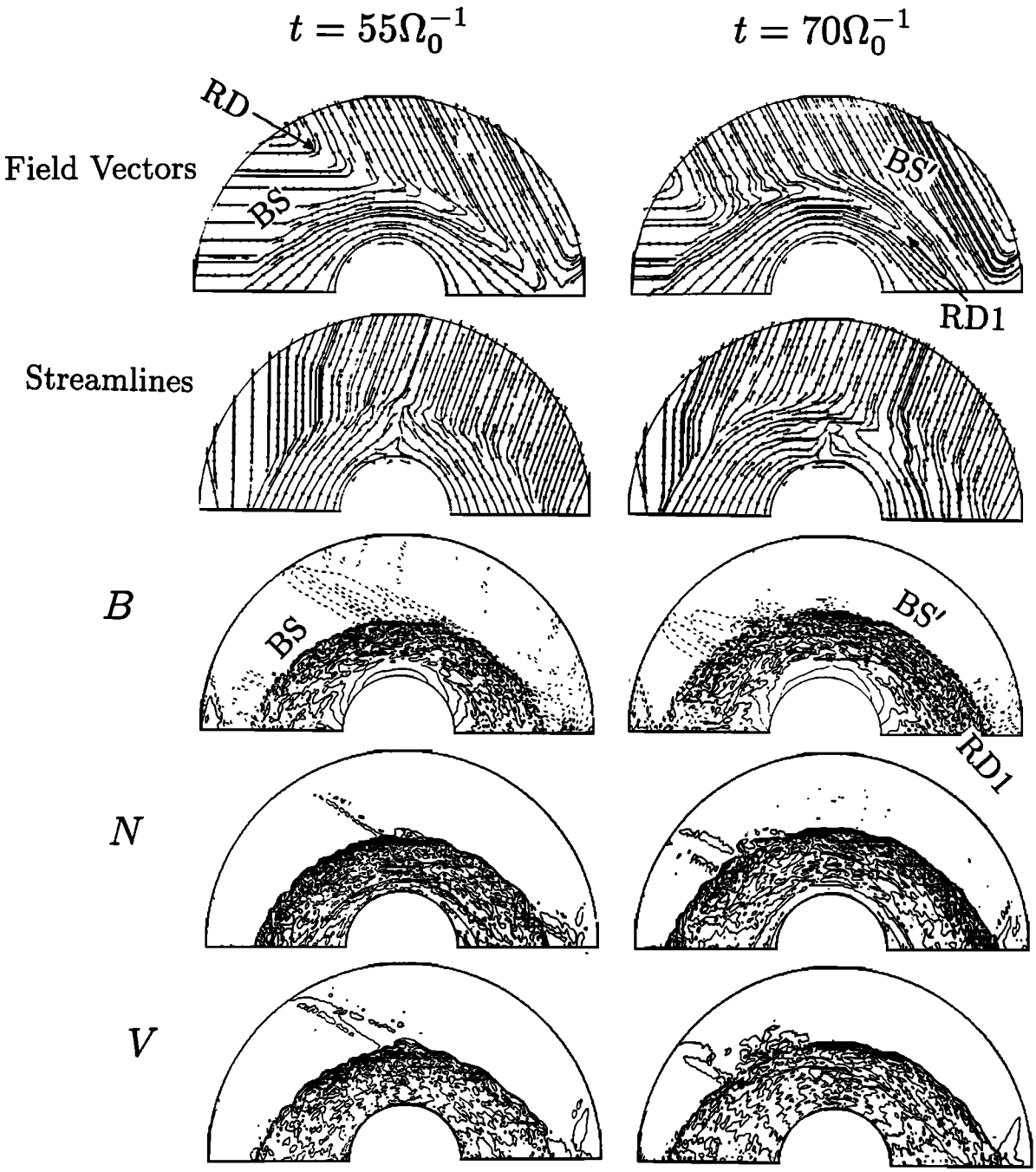

Figure 10. Magnetic field vectors, streamlines, and contours of magnetic field, ion number density, and flow speed at $t = 55\ \Omega_0^{-1}$ and $70\ \Omega_0^{-1}$ obtained in case 7.

the incoming TD. A strong sunward deflection in ion flow velocity may be present in the upstream bulge as well as in the downstream magnetosheath. The formation of the bulge and the anomalous flows is found to depend on the direction and symmetry condition of the upstream motional electric field:

(1) In the cases with a symmetric normal component of electric field on the two sides of the incoming TD, the bulge may be formed under a electric field which causes the reflected ions to be focused toward the current sheet. The bulge is generated by the reflected ions moving upstream from the trailing edge of the TD. On the other hand, in the cases with a electric field pointing away from the TD, the bulge is less likely to be formed in the upstream. These results seem to be consistent with the previous studies by *Burgess* [1989] and *Thomas et al.* [1991].

(2) In the cases with an asymmetric electric field or asymmetric B_z on the two sides of TD, the formation of the bulge is found to be due to two additional reasons with or without a proper sense of electric field. First, it is formed when the total pressure is unbalanced near the intersection of the BS and TD, which is caused by the sunward or earthward shift of the modified bow shock

BS′ relative to the original BS. The reflected ions also cause the reformation of the bow shock. As a result, the downstream plasma expands to its low pressure ambient as well as to the sunward upstream. An unequal ion density and field across the interplanetary TD may enhance the bulge and thus the flow deflection. Second, local magnetic reconnections may also be an important reason for the sunward deflection of the flow. As the interplanetary current sheet collides with the bow shock, the current sheet is compressed, and disturbances are present in the TD. A magnetic reconnection may be developed at the intersection between the BS and the TD. The field tension force associated with the X line may then accelerate the plasma to the upstream. The reconnection is found to be more significant when the field rotation angle $\Delta\Phi_B$ is larger than 80°.

While our simulation shows that the anomalous flows may be present for both proper and improper electric fields, a further study for the structure of the bulges under various directions and symmetry conditions of the electric field on the two sides of the TD [e.g., *Thomsen et al.*, 1993] has not been conducted.

The spatial profiles of physics quantities through the bulge are found to be consistent with the satellite crossings near the bow shock [e.g., *Thomsen et al.*, 1986, 1988; *Paschmann et al.*, 1988; *Schwartz et al.*, 1988] in many aspects. A strong density and field enhancement is found to flank the bulge, while a core plasma region with low density is present in the event. The thickness and strength of the boundary which contains the high field and density vary with the location across the bulge, and so do the values of the low density inside the events. In later phases of the bulge expansion, a low magnetic field may also be present in the core of the bulge. A high ion temperature which is comparable to the downstream temperature is found in the bulge region. The magnetic field direction changes at the bulge, whereas in our simulation this change is usually present near the leading egde of the bulge. The solar wind flow speed becomes subsonic in the bulge. The presence of the bulge at the bow shock has been suggested by *Schwartz et al.* [1988] for the generation of the observed anomalous flow events at the bow shock. For a typical IMF in the Parker spiral, such flow events are more likely to appear in the dawn side flank region.

In the interaction of the BS with an interplanetary RD, a structure RD1 that consists of slow modes and rotational discontinuities is generated in the magnetosheath. Across RD1, the magnetic field rotates by nearly the same angle as across the initial RD. The plasma may be accelerated or decelerated by the field tension force associated with the kinked field in RD1, and a flow deflection is present in the magnetosheath. A strong sunward deflection in the flow may be found for the interaction of BS with an RD whose propagation direction is oblique to the Sun-Earth line. Our simulation results suggest that an anomalous flow event in the magnetosheath may be generated by a BS/RD interaction. A significant sunward deflection in the ion flow may require a large $\Delta\Phi_B$ in the interplanetary RD.

As discussed in section 3, there are some features of the observed bulge that are not found in our simulation. For example, an isotropic ion velocity distribution in the hot flow anomaly near upstream of the bow shock [e.g., *Thomsen et al.*, 1986] is not found in the simulation. Instead, the perpendicular temperature is usually much higher than the parallel temperature. There is also a slow upstream propagation of the bow shock in our simulation. Further study including the 3-D effects on the BS/discontinuity interaction and more realistic time scales and spatial scales associated with the bow shock may be needed. Furthermore, the arrival of the resulting TD′ and RD1 at the magnetopause and its effects on the flow structure in the bow shock and magnetosheath are not studied in our simulation. In addition, the arrival of hot diamagnetic cavities at the magnetopause may produce strong effects on the magnetosphere. Such studies would also require a 3-D model in which the incoming magnetic fluxes can be removed from the dayside magnetopause in a self-consistent way.

Acknowledgments. The author would like to thank C. J. Farrugia for explaining the observations of the anomalous flow events associated with active solar wind current sheets. She is also grateful to S. J. Schwartz for drawing her attention to some related previous work on this subject. This work was supported by ONR grant NAVY-N00014-951-0839 and NSF grant ATM-9507993 to the Auburn University. Computer resources were provided by the San Diego Supercomputer Center and the Arctic Region Supercomputer Center.

The Editor thanks S. J. Schwartz and another referee for their assistance in evaluating this paper.

References

Behannon, K. W., F. M. Neubauer, and H. Barnstorf, Fine-scale characteristics of interplanetary sector boundaries, *J. Geophys. Res., 86*, 3273, 1981.

Brunelli, B. E., and S. A. Grib, Interaction of solar wind shock waves with the Earth's magnetosphere, *NASA Tech. Transl. NAS3-2481*, 37 pp., 1973.

Burgess, D., On the effects of a tangential discontinuity on ions specularly reflected at an oblique shock, *J. Geophys. Res., 94*, 472, 1989.

Burgess, D., and S. J. Schwartz, Colliding plasma structures: Current sheet and perpendicular shock, *J. Geophys. Res., 93*, 11,327, 1988.

Burlaga, L. F., Hydromagnetic waves and discontinuities in the solar wind, *Space Sci. Rev., 12*, 600, 1971.

Burlaga, L. F., and N. F. Ness, Tangential discontinuities in the solar wind, *Sol. Phys., 9*, 467, 1969.

Burlaga, L. F., and K. W. Ogilvie, Causes of sudden commencements and sudden impulses, *J. Geophys. Res., 74*, 2815, 1969.

Cahill, L. J., and V. L. Patel, The boundary of the geomagnetic field, August to November 1961, *Planet. Space Sci., 15*, 997, 1967.

Cargill, P. J., and T. E. Eastman, The structure of tangential discontinuities, 1, Results of hybrid simulations, *J. Geophys. Res., 96*, 13,763, 1991.

Chao, J. K., and R. L. Lepping, A correlative study of ssc's, interplanetary shocks, and solar activity, *J. Geophys. Res., 79*, 1799, 1974.

Chao, J. K., and S. Olbert, Observation of slow shocks in interplanetary space, *J. Geophys. Res., 75*, 6394, 1970.

Dryer, M., Bow shock and its interaction with interplanetary shocks, *Radio Sci., 8*, 893, 1973.

Gogosov, V. V., Resolution of an arbitrary discontinuity in magnetohydrodynamics, *J. Appl. Math. Mech., 25*, 148, 1961.

Gosling, J. T., D. J. McComas, J. L. Phillips, L. A. Weiss, V. J. Pizzo, B. E. Goldstein, and R. J. Forsyth, A new class of forward-reverse shock pairs in the solar wind, *Geophys. Res. Lett., 21*, 2271, 1994.

Hassam, A. B., Transmission of Alfven waves through the Earth's bow shock: Theory and observation, *J. Geophys. Res., 83*, 643, 1978.

Jeffrey, A., and T. Taniuti, *Nonlinear Wave Propagation With Application to Physics and Magnetohydrodynamics*, Academic, San Diego, Calif., 1964.

Landau, L. D., and E. M. Lifshitz, *Electrodynamics of Continuous Media*, Pergamon Tarrytown, N. Y., 1960.

Lee, L. C., L. Huang, and J. K. Chao, On the stability of rotational discontinuities and intermediate shocks, *J. Geophys. Res., 94*, 8813, 1989.

Leroy, M. M., and D. Winske, Backstreaming ions from oblique Earth bow shocks, *Ann. Geophys., 1*, 527, 1983.

Lin, Y., and L. C. Lee, Structure of the dayside reconnection layer in resistive MHD and hybrid model, *J. Geophys. Res., 98*, 3919, 1993.

Lin, Y., L. C. Lee, and M. Yan, Generation of dynamic pressure pulses downstream of the bow shock by variations in the interplanetary magnetic field orientation, *J. Geophys. Res., 101*, 479, 1996a.

Lin, Y., D. W. Swift, and L. C. Lee, Simulation of pressure pulses in the bow shock and magnetosheath driven by variations in interplanetary magnetic field direction, *J. Geophys. Res., 101*, 27,251, 1996b.

Mandt, M. E. and L. C. Lee, Generation of Pc 1 waves by the ion temperature anisotropy associated with fast shocks caused by sudden impulses, *J. Geophys. Res., 96*, 17,897, 1991.

Neubauer, F. M., Nonlinear oblique interaction of interplanetary tangential discontinuities with magnetogasdynamic shocks, *J. Geophys. Res., 80*, 1213, 1975.

Neubauer, F. M., Nonlinear interaction of discontinuities in the solar wind and the origin of slow shocks, *J. Geophys. Res., 81*, 2248, 1976.

Neugebauer, M., D. R. Clay, B. E. Goldstein, B. T. Tsurutani, and R. D. Zwickl, A reexamination of rotational and tangential discontinuities in the solar wind, *J. Geophys. Res., 89*, 5395, 1984.

Onsager, T. G., M. F. Thomsen, and D. Winske, Hot flow anomaly formation by magnetic deflection, *Geophys. Res. Lett., 17*, 1621, 1990.

Paschmann, G., G. Haerendel, N. Sckopke, E. Mobius, H. Luhr, and C. W. Carlson, Three-dimensional plasma structures with anomalous flow directions near the Earth's bow shock, *J. Geophys. Res., 93*, 11,279, 1988.

Richter, A. K., and M. Scholer, on the stability of rotational discontinuities, *Geophys. Res. Lett., 16*, 1257, 1989.

Richter, A. K., H. Rosenbauer, F. M. Neubauer, and N. G. Ptitsyna, Solar wind observations associated with a slow forward shock waves at 0.31 AU, *J. Geophys. Res., 90*, 7581, 1985.

Russell, C. T., J. T. Gosling, R. D. Zwickl, and E. J. Smith, Multiple spacecraft observations of interplanetary shocks: ISEE three-dimensional plasma measurements, *J. Geophys. Res., 88*, 9941, 1983.

Scholer, M., and T. Terasawa, Ion reflection and dissipation at quasi-parallel collisionless shocks, *Geophys. Res. Lett., 17*, 119, 1990.

Schwartz, S. J., Hot flow anomalies near the Earth's bow shock, *Adv. Space Res., 15(8/9)*, 107, 1995.

Schwartz, S. J., et al., An active current sheet in the solar wind, *Nature, 318*, 269, 1985.

Schwartz, S. J., R. L. Kessel, C. C. Brown, L. J. C. Woolliscroft, M. W. Dunlop, C. J. Farrugia, and D. S. Hall, Active current sheets near the Earth's bow shock, *J. Geophys. Res., 93*, 11,295, 1988.

Shen, W. W., and M. Dryer, Magnetohydrodynamic theory for the interaction of an interplanetary double-shock ensemble with the Earth's bow shock, *J. Geophys. Res., 77*, 4627, 1972.

Song, P., C. T. Russell, and M. F. Thomsen, Slow mode transition in the frontside magnetosheath, *J. Geophys. Res., 97*, 8295, 1992.

Swift, D. W., Use of a hybrid code to model the Earth's magnetosphere, *Geophys. Res. Lett., 22*, 311, 1995.

Swift, D. W., Use of a hybrid code for a global-scale plasma simulation, *J. Comput. Phys., 126*, 109, 1996.

Swift, D. W., and L. C. Lee, Rotational discontinuities and the structure of the magnetopause, *J. Geophys. Res., 88*, 111, 1983.

Thomas, V. A., and S. H. Brecht, Evolution of diamagnetic cavities in the solar-wind, *J. Geophys. Res., 93*, 11,341, 1988.

Thomas, V. A., D. Winske, M. F. Thomsen, and T. G. Onsager, Hybrid simulation of the formation of a hot flow anomaly, *J. Geophys. Res., 96*, 11,625, 1991.

Thomsen, M. F., J. T. Gosling, S. A. Fuselier, S. J. Bame, and C. T. Russell, Hot, diamagnetic cavities upstream from the Earth's bow shock, *J. Geophys. Res., 91*, 2961, 1986.

Thomsen, M. F., J. T. Gosling, S. J. Bame, K. B. Quest, C. T. Russell, and C. T. Fuselier, On the origin of hot diamagnetic cavities near the Earth's bow shock, *J. Geophys. Res., 93*, 11,311, 1988.

Thomsen, M. F., V. A. Thomas, D. Winske, J. T. Gosling, M. H. Farris, and C. T. Russell, Observational test of hot flow anomaly formation by the interaction of a magnetic discontinuity with the bow shock, *J. Geophys. Res., 98*, 15,319, 1993.

Volk, H. J., and R. D. Auer, Motions of the bow shock induced by interplanetary disturbances, *J. Geophys. Res., 79*, 40, 1974.

Whang, Y. C., J. Zhou, R. P. Lepping, and K. W. Ogilvie, Interplanetary slow shock observed by WIND, *Geophys. Res. Lett., 23*, 1239, 1996.

Wu, B. H., M. E. Mandt, L. C. Lee, and J. K. Chao, Magnetospheric response to solar wind dynamic pressure variations: Interaction of interplanetary tangential discontinuities with the bow shock, *J. Geophys. Res., 98*, 21,297, 1993.

Yan, M., and L. C. Lee, Generation of slow-mode waves in front of the dayside magnetopause, *Geophys. Res. Lett., 21*, 629, 1994.

Yan, M., and L. C. Lee, Interaction of interplanetary shocks and rotational discontinuities with the Earth's bow shock, *J. Geophys. Res., 101*, 4835, 1996.

Y. Lin, Physics Department, Auburn University, 206 Allison Laboratory, Auburn, AL 36849-5311. (e-mail: ylin@physics.auburn.edu)

(Received February 28, 1997; revised July 8, 1997; accepted July 9, 1997.)